Spin reorientation and magnetoelastic properties of ferromagnetic $Tb_{1-x}Nd_xCo_2$ systems with a morphotropic phase boundary

Adil Murtaza,[1] Sen Yang,[1,*] Tieyan Chang,[1] Awais Ghani,[1] Muhammad Tahir Khan,[1] Rui Zhang,[1] Chao Zhou,[1] Xiaoping Song,[1] Matthew Suchomel,[2] and Yang Ren[2]

[1]*School of Science, MOE Key Laboratory for Nonequilibrium Synthesis and Modulation of Condensed Matter, State Key Laboratory for Mechanical Behavior of Materials, Xi'an Jiaotong University, Xi'an 710049, China*
[2]*X-Ray Science Division, Argonne National Laboratory, Argonne, Illinois 60439, USA*

The spin reorientation (SR) and magnetoelastic properties of pseudobinary ferromagnetic $Tb_{1-x}Nd_xCo_2$ ($0 \leqslant x \leqslant 1.0$) systems involving a morphotropic phase boundary (MPB) were studied by high-resolution synchrotron x-ray diffraction (XRD), magnetization, and magnetostriction measurements. The easy magnetization direction of the Laves phase lies along the $\langle 111 \rangle$ axis with $x < 0.65$, whereas it lies along the $\langle 100 \rangle$ axis for $x > 0.65$ below Curie temperature (T_C). The temperature-dependent magnetization curves showed SR; this can be explained by a two-sublattice model. Based on the synchrotron (XRD) and magnetization measurements, the SR phase diagram for a MPB composition of $Tb_{0.35}Nd_{0.65}Co_2$ was obtained. Contrary to previously reported ferromagnetic systems involving MPB, the MPB composition of $Tb_{0.35}Nd_{0.65}Co_2$ exhibits a low saturation magnetization (M_S), indicating a compensation of the Tb and Nd magnetic moments at MPB. The anisotropic magnetostriction (λ_S) first decreased until $x = 0.8$ and then continuously increased in the negative direction with further increase of Nd concentration. The decrease in magnetostriction can be attributed to the decrease of spontaneous magnetostriction λ_{111} and increase of λ_{100} with opposite sign to λ_{111}. This paper indicates an anomalous type of MPB in the ferromagnetic $Tb_{1-x}Nd_xCo_2$ system and provides an active way to design novel functional materials with exotic properties.

I. INTRODUCTION

In recent years, magnetically ordered materials with both magnetic and structural phase transitions have drawn special attentions owing to their novel physical properties and possible applications in advanced technologies [1–5]. Rare-earth (RE) compounds with Laves phases $RECo_2$ are quite interesting in condensed-matter physics due to their simple magnetic and crystallographic structures to validate different physical models [4,6–8]. These are potential candidates to study different properties such as magnetoelastic, magnetocaloric, and magnetoelectric phenomena because of large magnetostriction, magnetocaloric effect, and magnetoresistance, respectively [3,4].

To exploit large magnetostriction for practical applications, it is necessary to minimize the magnetocrystalline anisotropy. Previous studies show that to decrease the anisotropy while maintaining a large magnetostriction, RE elements such as Dy, Gd, and Ho were substituted with Tb in $TbCo_2$, affording the corresponding pseudobinary ferromagnetic compounds $Tb_{1-x}Dy_xCo_2$, $Tb_{1-x}Gd_xCo_2$, and $Tb_{1-x}Ho_xCo_2$, respectively [9,10]. These ferromagnetic systems possess a specific feature: morphotropic phase boundary (MPB), a boundary where two ferromagnetic phases with different crystallographic symmetries are abruptly separated in the composition-temperature phase diagram similar to ferroelectrics [11–15]. Near the MPB region, the free-energy landscape allows the

polarization to rotate easily, resulting in an enhanced functional response.

In previously reported ferromagnetic $Tb_{1-x}Dy_xCo_2$ systems involving MPB, the MPB composition of $x = 0.7$ shows a peak in the magnetic susceptibility and magnetostrictive figure of merit as well as a minimum in the coercive field. The boundary between rhombohedral and tetragonal phases is magnetoelastic, as first reported in Ref. [14]. Zhou *et al.* reported magnetoelastic properties in a ferromagnetic $Tb_{1-x}Gd_xCo_2$ system, where the MPB composition of $x = 0.9$ shows a large magnetization and low (near zero) magnetostriction [15]. In these ferromagnetic systems involving MPB, the end members of the composition-temperature phase diagram have different easy magnetization directions (EMDs) below Curie temperature (T_C) to accomplish the weakening of magnetization anisotropy at MPB, thus facilitating the magnetic domain switching.

Based on the same mechanism, we designed MPB in a ferromagnetic $Tb_{1-x}Nd_xCo_2$ system, in which the EMD of $TbCo_2$ lies along the $\langle 111 \rangle$ axis below $T_C \sim 230$ K and the EMD of $NdCo_2$ lies along the $\langle 100 \rangle$ axis below $T_C \sim 100$ K [16,17]. Therefore, it is expected that the $Tb_{1-x}Nd_xCo_2$ system with an appropriate composition has a small magnetic anisotropy and different EMDs, although in earlier studies the mixing effects of light and heavy RE in the Laves phase $Tb_{1-x}Nd_xCo_2$ compounds were investigated by x-ray diffraction (XRD) and magnetic measurements. Structural distortion and change of EMD were observed by conventional diffractometry with a low resolution of characteristic (440) reflections only. It was shown that the EMD of the $Tb_{1-x}Nd_xCo_2$ system changes

*yang.sen@mail.xjtu.edu.cn

from $\langle 111 \rangle$ axis to $\langle 100 \rangle$ axis between $x = 0.6$ and 0.7 [2,16]. Magnetization measurements revealed that the compounds exhibit a field-induced metamagnetic transition from a strong ferrimagnetism to a weak ferrimagnetism near $x = 0.6$ at 5 K. Within the assumption of a linear variation of the magnetic moment of the RE sublattice, it was concluded that such an anomalous magnetic moment is due to abrupt change of the Co moment [18,19]. However, some of the features of the ferromagnetic $Tb_{1-x}Nd_xCo_2$ system, which were not considered previously, are explored in the present paper. We designed a MPB in the $Tb_{1-x}Nd_xCo_2$ system and discovered another case: with the concentration change from the end member of the rhombohedral phase (R) to that of the tetragonal phase (T), the value of maximum magnetostriction changes, but the value of magnetization achieves the minimum at MPB composition. By using high-resolution synchrotron XRD, a detailed analysis of the characteristic (222), (440), and (800) reflections was carried out. We have shown direct evidence that the ferromagnetic $Tb_{1-x}Nd_xCo_2$ system with critical composition $x_c = 0.65$ is a mixture of two phases (i.e., R phase and T phase), corresponding to MPB. A detailed composition-temperature-dependent phase diagram around MPB composition is given. Field-dependent magnetization (M-H) reveals that the MPB composition has lower coercivity at low field ($H = 0.8$ kOe) and a high coercivity at high field ($H = 12$ kOe). Based on our experimental results, a figure of merit is constructed, exhibiting the peak value at MPB. Ouyang *et al.* showed that the magnetization and anisotropy constant in $Tb_{1-x}Nd_xCo_2$ exhibit a minimal value between $x = 0.6$ and 0.7 at a low temperature of 5 K [18]. The temperature-dependent magnetization (M-T) curves and composition-temperature-dependent phase diagram of $Tb_{1-x}Nd_xCo_2$ reveal that such a low temperature of 5 K corresponds to an orthorhombic O phase instead of R phase, and T phase, or MPB region. As the MPB composition $x_c = 0.65$ corresponds to the coexistence of R phase and T phase in the temperature range from 20 to 150 K, it is important to measure the magnetization and anisotropy constant of MPB composition $x_c = 0.65$ at 90 K. Despite the similarity with previously reported MPB involved ferromagnetic $Tb_{1-x}Dy_xCo_2$, $Tb_{1-x}Gd_xCo_2$ systems and the same easy-domain-switching feature at MPB, the ferromagnetic $Tb_{1-x}Nd_xCo_2$ system shows a low magnetization at the MPB composition $x_c = 0.65$ compared to the known ferromagnetic materials involving MPB. The present paper shows an anomalous type of MPB in ferromagnetic materials, revealing that MPB can also lead to weakening of magnetoelastic behavior as shown in the ferromagnetic $Tb_{1-x}Nd_xCo_2$ system.

II. EXPERIMENTAL PROCEDURES

The $Tb_{1-x}Nd_xCo_2$ ($0 \leqslant x \leqslant 1.0$) samples were prepared by arc-melting method using the raw materials Tb (99.9%), Nd (99.9%), and Co (99.9%) under argon atmosphere. Each sample was melted several times to ensure homogeneity, and the as-casted samples were annealed at 700 °C under vacuum for ten days. High-resolution synchrotron XRD experiments were performed to determine the crystal symmetry. For this synchrotron XRD analysis, a small amount of the samples was ground into powders and sealed in quartz capillaries with a diameter of 0.3 mm at beamline 11-IDC, Advanced

Photon Source, Argonne National Laboratory, USA. The wavelength of the synchrotron x ray was 0.11725 Å. During the synchrotron XRD measurement, the capillary was rotated to average the intensity and to reduce the preferred orientation effect. The Curie temperatures were determined by magnetization (M) versus temperature (T) measured by using a vibrating sample magnetometer. The magnetization (M) versus magnetic field (H) hysteresis loops were measured by using a Quantum Design superconducting quantum interference device (SQUID) magnetometer, and the magnetostriction was measured at 90 K under a field of 10 kOe by using the standard strain-gauge technique with a gauge factor of $2.11 \pm 1\%$.

III. RESULTS AND DISCUSSION

A. Crystal symmetry and lattice distortion

The synchrotron XRD profiles at 300 and 90 K are shown in Figs. 1(a) and 1(b), respectively. The XRD profiles show that at 300 K the characteristic reflections of (222), (440), and (800) show no splitting and can be fitted by using a single peak as shown in Fig. 1(a). These features characterize a cubic structure for the ferromagnetic $Tb_{1-x}Nd_xCo_2$ system. However, at 90 K for compositions of $x = 0$ and 0.5, the characteristics reflections of (222) and (440) can be fitted by using double peaks, indicating a splitting in the (222) and (440) reflections. However, the characteristic (800) reflections show no splitting and can be fitted by using a single peak [Fig. 1(b)]; these are the characteristics of EMD along the $\langle 111 \rangle$ axis corresponding to the rhombohedral symmetry. All the characteristic reflections of the compounds slightly shifted to the lower Bragg's angles, and the splitting became weaker with increasing Nd content. For compositions $x = 0.7$ and 1.0, the characteristic (222) and (440) peaks can be fitted by using a single peak, indicating no splitting in (222) and (440) reflections. However, the characteristic splitting in (800) reflections can be fitted by using double peaks. This indicates the splitting in (800) reflections as shown in Fig. 1(b), signifying that the EMD along the $\langle 111 \rangle$ axis corresponds to the tetragonal symmetry. For the critical composition of $x_c = 0.65$, the XRD profiles show that the characteristic (222), (440), and (800) reflections can be fitted by using double peaks, indicating splitting in (222), (440), and (800) reflections. The critical composition $x_c = 0.65$ behaves as a structural bridge between the rhombohedral and tetragonal symmetries. It is known that a spontaneous magnetostriction of compounds with the $MgCu_2$-type Laves phase leads to structural distortion. When the EMD lies along $\langle 111 \rangle$ or $\langle 100 \rangle$ axes, a large rhombohedral or tetragonal distortion occurs, respectively, resulting in the splitting of characteristic (440) reflection [20]. Thus, the (440) reflection in the XRD patterns is doubly split when the EMD lies along the $\langle 111 \rangle$ axis, while a single peak is maintained when the EMD lies along the $\langle 100 \rangle$ axis.

B. Magnetostrictive coefficients

For RE transition-metal (TM) compounds ($RETM_2$) with Laves phases, a close correlation was observed between the EMD and the crystallographic symmetry of the distorted Laves phases [21]. Previously reported data showed that the splitting of rhombohedrally distorted cubic reflections can be used to
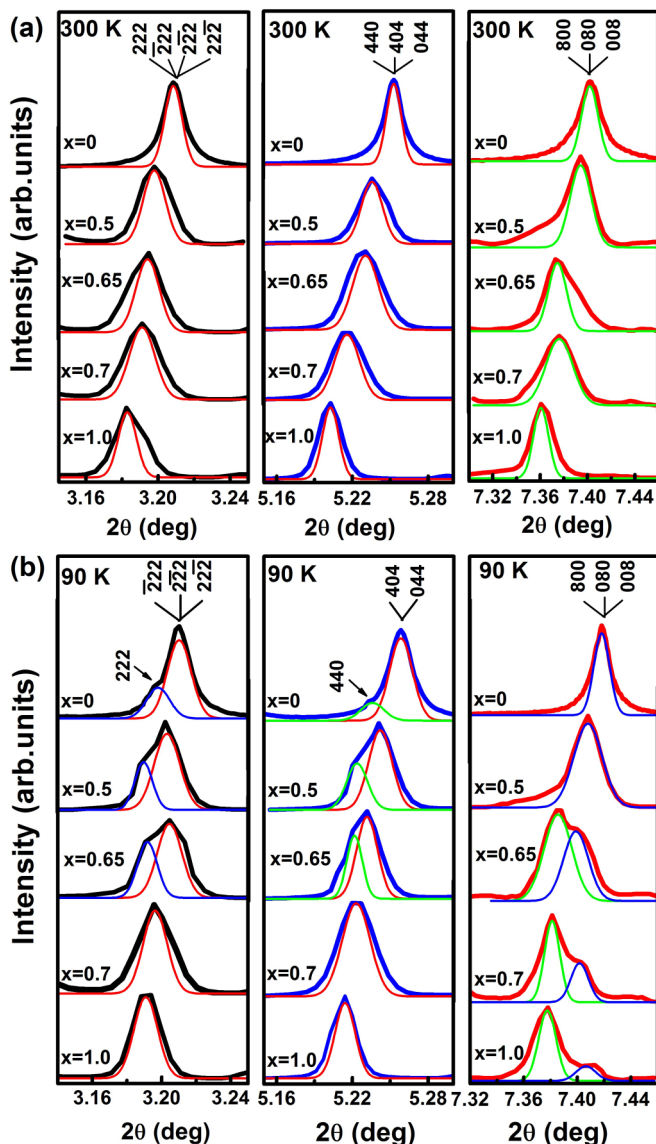
FIG. 1. Synchrotron XRD patterns (typical 222, 440, and 800 peaks) of $Tb_{1-x}Nd_xCo_2$ for $x = 0$, 0.5, 0.65, 0.7, and 1.0 with a wavelength of 0.11725 Å at (a) 300 K and (b) 90 K.
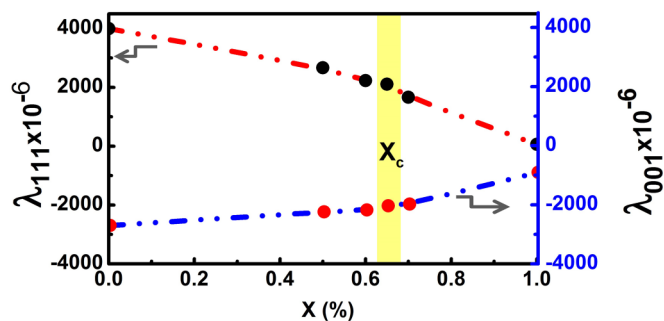

FIG. 2. Composition dependence of magnetostriction coefficients λ_{111} and λ_{100} for $Tb_{1-x}Nd_xCo_2$. The yellow shaded area corresponds to MPB.

determine the magnetostrictive coefficient (λ_{111}) [22,23]. As MPB corresponds to the coexistence of rhombohedral and tetragonal phases, magnetostriction at the MPB is contributed by both the rhombohedral (λ_{111}) and tetragonal (λ_{100}) distortions. In the $RETM_2$ Laves phase, the EMD of the mixture of compounds is the same as that of the predominant RE element [24]. Therefore, for the Tb-rich side ($x < 0.65$), the splitting of (222) reflections is mainly contributed by the rhombohedral distortion. With the increase of Nd concentration, the rhombohedral distortion decreases and disappears at the Nd-rich side. For the Nd-rich side ($x > 0.65$), the tetragonal distortion results in the splitting of (800) reflections as shown in Fig. 1(b). Thus, in this paper, we used the characteristic (222) and (800) peak splitting to calculate the λ_{111} and λ_{100} values for $Tb_{1-x}Nd_xCo_2$.

The calculated magnetostriction coefficients λ_{111} and λ_{100} show that with increasing Nd concentration the λ_{111} decreased,

while the λ_{100} increased, as shown in Fig. 2. As a large anisotropic magnetostriction, $\lambda_{111} \gg \lambda_{100}$ is a typical characteristic of $REFe_2$ compounds. Previously reported coefficients (λ_{111}, λ_{100}) showed that a very small λ_{100} originates from the Fe sublattice, whereas $RECo_2$ has large λ_{111} and λ_{100} simultaneously, originating from the RE and Co sublattices, respectively [8]. It is well known that the natures of Fe or Co ions in $REFe_2$ or $RECo_2$ differ from each other. Fe has an intrinsic moment, whereas Co has an induced moment. Co significantly contributes to the anisotropic magnetostriction compared to RE, whereas this is not the case for Fe. The substitution of Fe in the ferromagnetic $Tb_{0.33}Nd_{0.67}(Co_{1-x}Fe_x)_2$ system dilutes the contribution of Co and leads to an increase of the ordering temperature accompanied by the appearance of room-temperature magnetostriction. Thus the competition of the Fe and Co sublattice anisotropies changes the anisotropy of the compounds and leads to the complex concentration dependence of the spontaneous magnetostriction λ_{111} [25]. The large λ_{100} was also observed in $RECo_2$ compounds, indicating that the large magnetoelastic deformation along the $\langle 100 \rangle$ axis in $RECo_2$ compounds is caused by the d-band system [20]. According to the structural distortion model proposed by Clark, only the TMs contribute to λ_{100} [26]. Therefore, an increase of λ_{100} in the $Tb_{1-x}Nd_xCo_2$ system is caused by Co.

C. Temperature-dependent magnetization ($M - T$) and spin reorientation diagram

The temperature-dependent magnetization (M-T) curves for various compositions of $Tb_{1-x}Nd_xCo_2$ ($0 \leqslant x \leqslant 1.0$) were measured in zero-field-cooled (ZFC) and field-cooled (FC) modes as shown in Fig. 3. In the ZFC mode, the sample is cooled in a zero applied dc magnetic field through its critical temperature (T_C), and the magnetization is recorded while warming the sample in the presence of a magnetic field. This mode of magnetization measurement is different from the FC magnetization measurements. In the FC mode, the sample is cooled through the critical temperature while applying a magnetic field and the FC magnetization is measured while warming the sample after the cooling [26]. The M-T curves show that the T_C decreased from 230 K for $x = 0$ to 100 K for $x = 1.0$. These values agree well with the previously reported data [16,17]. The decrease in T_C indicates a stronger coupling between Tb and Co than that between Nd and Co.
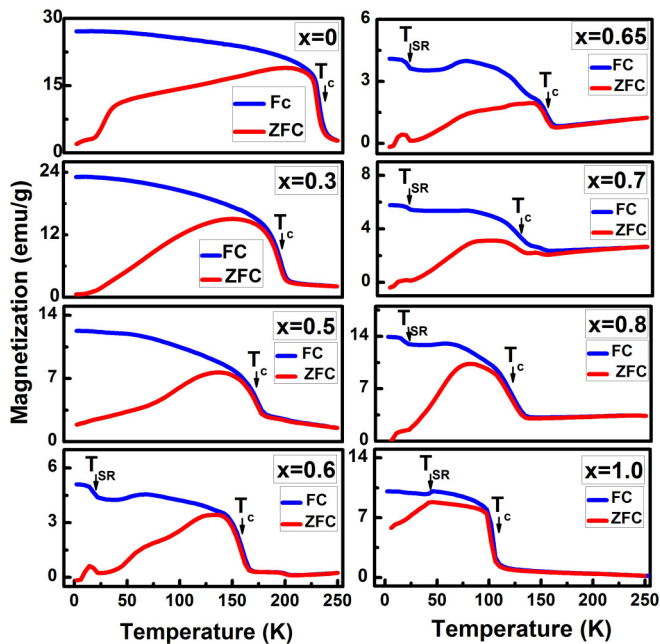
FIG. 3. ZFC and FC temperature dependence of magnetization (M-T) curves of the Tb$_{1-x}$Nd$_x$Co$_2$ system ($x = 0$, 0.3, 0.5, 0.6, 0.65, 0.7, 0.8, and 1.0) measured under an applied magnetic field of 500 Oe.

The M-T curves show that the spin reorientation (SR) for $x = 0.6$ corresponds to the ferro-ferro transition temperatures denoted by T_{SR}. Figure 3 shows that the transition temperature corresponding to the peak decreased with increasing Nd concentration. The presence of SR can be explained by the two-sublattice model [27,28]. This model simply considers the total magnetization as a vector sum of the magnetizations of RE and TM sublattices which interact via the RE-TM exchange coupling between the two sublattices. The RE-TM spin-exchange coupling has an antiferromagnetic character and leads to a parallel $3d$ and $4f$ moment configuration for the light RE elements and to an antiparallel moment configuration for the heavy RE elements. It is well known that magnetic anisotropy (K_1) can also affect the relative orientation of sublattice magnetizations. Usually, the RE-TM interaction is dominant because it is very strong compared to the magnetic anisotropy. The magnetic anisotropy arises from the coupling of the magnetic moments of the RE and TM atoms in the crystal lattice [29]. In most compounds, especially at low temperatures, the magnetic anisotropy of the RE sublattice is stronger than that of the TM sublattice [30]. However, in some cases, the magnetic anisotropies of the two sublattices are comparable in magnitude and may compete in determining the nature of the net anisotropy of the compound. Following the two-sublattice model, the RE sublattice anisotropy and TM sublattice magnetic anisotropy may favor different EMDs.

With decreasing temperature, the occurrence of SR accompanies the appearance of nonmajor symmetry axes of the EMD. Owing to different temperature dependences of the anisotropies of the two sublattices, the competing RE and TM anisotropies could change the EMD of the compounds, leading to a characteristic temperature dependence of the magnetization. The EMD reflects the dependence of the

magnetic free energy of crystallographic directions. Because of the continuous transition of EMD, the existence of unusual *<uvw>*- or *<uv0>*-type axes of easy magnetization can be interpreted by using the magnetic anisotropy energy [31] of

$$E(\vec{n}, T) = K_0 + K_1\left(a_x^2 a_y^2 + a_y^2 a_z^2 + a_z^2 a_x^2\right)$$
$$+ K_2\left(a_x^2 a_y^2 a_z^2\right) + \dots, \quad (1)$$

where a_x, a_y, and a_z are the direction cosines of the easy magnetic axes in the cubic lattice, and $\vec{n}$ is the direction of magnetization with respect to cubic axes and can be defined in terms of direction cosines as $\vec{n} = (a_x, a_y, a_z)$. K_1 and K_2 are the temperature-dependent magnetic anisotropy constants. Considering $a_x = \cos\alpha$, $a_y = \cos\beta$, and $a_z = \cos\gamma$ and the cosine relation $\cos^2\alpha + \cos^2\beta + \cos^2\gamma = 1$, the differentiation of $E(\vec{n}, T)$ with respect to the angles β and γ yields only the minima for a_i ($i = x, y, z$) corresponding to the major axes of symmetry of the cubic system, namely, the $\langle 111\rangle$, $\langle 110\rangle$, and $\langle 100\rangle$ directions. These become the easy axes of magnetization depending on the relative values of K_1 and K_2. Therefore, the possible condition for the minima in $E(\vec{n}, T)$ is

$$\frac{\partial E(\vec{n}, T)}{\partial \beta}, \ \frac{\partial E(\vec{n}, T)}{\partial \gamma} = 0. \quad (2)$$

EMD departs from the major axes of symmetry over a relatively wide temperature interval in which the magnetization vector rotates over a wide range of directions. These unusual directions of magnetization other than the major cubic axes are probably caused by the distortions of the cubic symmetry. The rotation of EMD can be confirmed by neutron-diffraction measurements [32]. For $x = 1.0$, NdCo$_2$ shows SR at $T_{SR} \approx$ 42 K, consistent with previously reported data as NdCo$_2$ undergoes a structural transition from the tetragonal phase to the orthorhombic phase at 42 K [8]. The magnetization curves show different behaviors under ZFC and FC. At low temperatures in the ZFC curve, the magnetization increases up to the SR temperature (T_{SR}). Above the SR temperature ($T > T_{SR}$) the magnetization increases and then continuous to decrease near the T_C, while in the FC curve at a low temperature the magnetization decreases up to a characteristic temperature (T_{SR}). Above the T_{SR}, the magnetization slightly increases for $x = 0.6$ and 0.65 and then decreases near the T_C. The distinct features of ZFC and FC measurements include a peak value in the ZFC and FC magnetization curve at a temperature (T_{SR}) and the ZFC and FC magnetization curves coincide at a high temperature.

Based on the analysis of synchrotron XRD data [Fig. 1] and temperature-dependent magnetization (M-T) [Fig. 3], the SR diagram for Tb$_{1-x}$Nd$_x$Co$_2$ was designed as shown in Fig. 4. Analysis of the SR diagram reveals that region I shows a paramagnetic cubic phase, while in region II the EMD lies along the $\langle 111\rangle$ axis and changes to the $\langle 100\rangle$ axis with increasing Nd concentration at $x_c = 0.65$ corresponding to region III. The transition of type $\langle 111\rangle \leftrightarrows \langle 100\rangle$ is a crystallographic phase transition between two different EMDs, i.e., from a rhombohedral symmetry (EMD//$\langle 111\rangle$) to a tetragonal symmetry (EMD//$\langle 100\rangle$) (regions II and III) as confirmed by the synchrotron XRD data [Fig. 1]. This composition-induced crystallographic phase transition is considered as the MPB phenomena in ferromagnetic systems, previously known as the SR
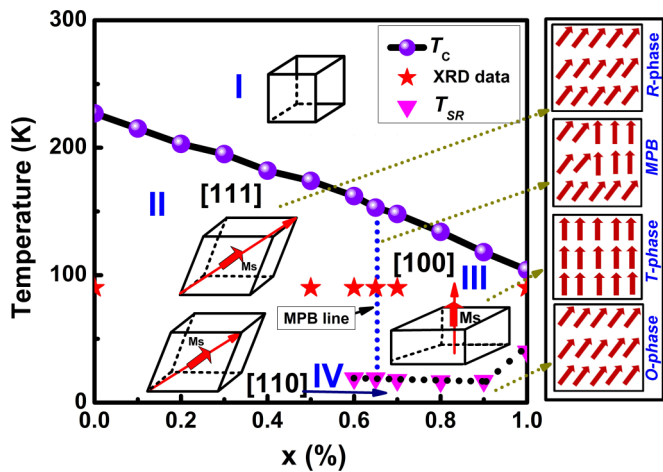
FIG. 4. SR diagram of $Tb_{1-x}Nd_xCo_2$ with cubic, rhombohedral, tetragonal, and orthorhombic crystal symmetries. Blue balls, red stars, and purple triangles denote the T_C points, synchrotron XRD data, and T_{SR}, respectively, while the blue dotted line shows the phase boundary between rhombohedral and tetragonal phases. Regions I, II, and III are deduced from the analysis of the results of synchrotron XRD data, and region IV is expected from the temperature dependence of magnetization. The inset on the right-hand side shows a schematic description of the SR process in R phase, T phase, and O phase and at MPB.

FIG. 5. Magnetic measurements. (a) The magnetization vs magnetic field (M-H) hysteresis loops for $Tb_{1-x}Nd_xCo_2$ at 90 K under an applied magnetic field of 0.8 and 12 kOe. Zoom hysteresis loops are shown in the insets. (b) Composition dependence of saturation magnetization (M_S), coercive fields (H_C), and magnetic anisotropy constant (K_1). The yellow shaded area in Fig. 5(b) corresponds to the critical composition of MPB.

transition (SRT) [11–13,19,30,33]. A schematic description of SRT from rhombohedral to tetragonal symmetry is shown in Fig. 4, also indicating that a SR, namely of type $\langle 111 \rangle \leftrightarrows \langle 110 \rangle$ or $\langle 100 \rangle \leftrightarrows \langle 110 \rangle$, takes place through a transition region as shown in region IV corresponding to the O phase.

D. Magnetic-field-dependent magnetization ($M - H$) and magnetic anisotropy

The field dependence of the magnetization (M-H) measured by using SQUID for $Tb_{1-x}Nd_xCo_2$ at 90 K under a magnetic field of 0.8 and 12 kOe is shown Fig. 5(a). The magnetization for all the compositions varies significantly, because the magnetizations of $TbCo_2$ and $NdCo_2$ are different. Further analysis shows that the magnetization curves do not saturate up to an applied field of 12 kOe; therefore, the saturation magnetization (M_S) was estimated following the law of approach to saturation [34]:

$$M = M_S \left[1 - \frac{a}{H} - \frac{b}{H^2} \right], \quad (3)$$

where M_S is the saturation magnetization; a and b are constants. The constant b is associated with anisotropy and can be derived from the law of saturation as follows:

$$b = \frac{8K_1^2}{105\mu_0^2 M_S^2}, \quad (4)$$

where K_1 is the first-order anisotropy constant and μ_o is the permeability of free space.

The composition dependence of saturation magnetization (M_S) is shown in Fig. 5(b). The M_S first decreases to a minimum value at the MPB composition $x_c = 0.65$ and then increases with the increase of Nd content. This behavior can
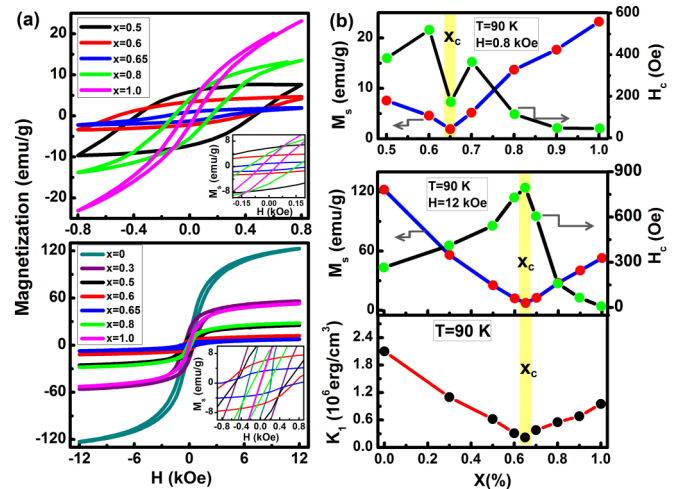
be interpreted by a two-sublattice model by compensating the sublattice magnetization [28,29].

Following the general rule of magnetic coupling between heavy or light RE and TM sublattices in $Tb_{1-x}Nd_xCo_2$, the Co moment was coupled parallel to the Nd moment and antiparallel to the Tb moment. In $Tb_{1-x}Nd_xCo_2$ for $x < 0.65$, the Tb-Co antiferromagnetic coupling is dominant, whereas the Nd-Co ferromagnetic coupling is dominant for $x > 0.65$ [35]. With the replacement of Nd with Tb, the magnetic moment of Tb decreases, thus decreasing the total magnetic moment and reaching a compensation point at MPB ($x_c = 0.65$). With further increase of Nd concentration, the contribution to the entire magnetization is mainly provided by the Nd atoms, leading to an increase in magnetization (M_S). The coercive field (H_C) determined from the hysteresis loops shows different behaviors under low and high fields as shown in Fig. 5(b). Under a low field (0.8 kOe), the MPB composition shows a lower coercive field between $x = 0.6$ and 0.7, while for a high magnetic field (12 kOe) the coercivity increases until the maximum value at MPB composition ($x_c = 0.65$) and then decreases with Nd concentration increasing as shown in Fig. 5(b). For ferromagnetic compounds, it is well known that a maximum of the coercive field exists near the compensation point, because the magnetic moment configuration does not change with field [36]. The composition dependence of coercive field (H_C) for this system is related to the saturation magnetization (M_S) and magnetic anisotropy (K) as $H_C \sim K/M_S$. Under a high magnetic field, MPB composition $x_c = 0.65$ shows the minimum magnetization; the above relation indicates that the MPB composition has a large coercive field (H_C). For a low magnetic field (0.8 kOe), although the MPB composition shows the minimum magnetization, according to the above relation, it should have a high coercive field. However, the experimental results show that at a low field

the MPB composition has a lower coercive field, indicating that at the MPB the anisotropy is low and magnetic moment can be easily switched under a low magnetic field. First-order magnetic anisotropy (K_1) calculated using Eq. (2) is shown in Fig. 5(b). At 90 K, the anisotropy decreases with increasing Nd concentration from $x = 0$ to $x_c = 0.65$ and beyond $x_c > 0.65$ it starts to increase. These results show a good agreement with the previously reported data, where M_S and K_1 at a very low temperature (5 K) possess a minimum value between $x = 0.6$ and 0.7 [34,36]. In the ferromagnetic $Tb_{1-x}Nd_xCo_2$ system, both the end members of the temperature-composition phase diagram have different anisotropies with different EMDs. The anisotropy of the $NdCo_2$ sublattice becomes dominant, resulting in anisotropy compensation at MPB composition $x_c = 0.65$, where the ferro-ferro transition occurs. Similar phenomena were also observed in ferroelectric MPB systems and attributed to the weakening polarization (strain) anisotropy while approaching MPB [12,13]. The anisotropy of the MPB composition $Tb_{0.35}Nd_{0.65}Co_2$ is smaller than that of the parent compound $TbCo_2$, because the dominant RE anisotropy of Tb is larger than that of Nd.

E. Anisotropic magnetostriction and figure of merit

The anisotropic magnetostriction (λ_S) of different compositions of $Tb_{1-x}Nd_xCo_2$ was measured under an applied field of up to 10 kOe as shown in Fig. 6(a). The results show that the magnetostriction first decreases until $x = 0.8$ and then continuously increases in the negative direction as the Nd content increases. The XRD data confirm that for $x \leqslant 0.8$ the c/a ratio is greater than unity, and the c direction of crystal elongates along the field direction and exhibits a positive magnetostriction (V-shaped curve) as shown in Fig. 6(a). For $x = 0.9$ and 1.0, the c/a ratio is less than unity, and the magnetostriction curves show contraction behavior under an external field, consistent with the Λ-like shape magnetostriction curve. This indicates that the c direction of crystal aligns with the external field. The ratio between magnetostriction and the absolute value of the first anisotropy constant (λ_S/K_1) is commonly used to demonstrate the merits of a magnetostrictive material [37]. The compositional dependence of the ratio λ_S/K_1 for $Tb_{1-x}Nd_xCo_2$ is shown in Fig. 6(b). Every curve shows a peak around the MPB composition $x_c = 0.65$ at different magnetic fields from 2 to 10 kOe. This result and the analysis of the synchrotron XRD and SR confirm that the anisotropy compensation could be achieved in $Tb_{1-x}Nd_xCo_2$ alloy. This confirms that the $Tb_{0.35}Nd_{0.65}Co_2$ system has a good low-field magnetostrictive property.

According to the single-ion model, the magnetostriction is proportional to the saturation magnetization of the RE sublattice M_{SR}^3. In analogy with the magnetization of $Tb_{1-x}Nd_xCo_2$, the magnetostriction does not maintain a minimum value at MPB. Therefore, the single-ion model is unable to explain the magnetostrictive behavior in this system.

The finding of MPB in the ferromagnetic $Tb_{1-x}Nd_xCo_2$ system has some important significances. It provides a better understanding of the fundamental concept of SRT such as the ferro-ferro transition between the R phase and T phase as shown in Fig. 4. Such transitions arise not only from the reorientation of magnetization but also from crystal symmetry change
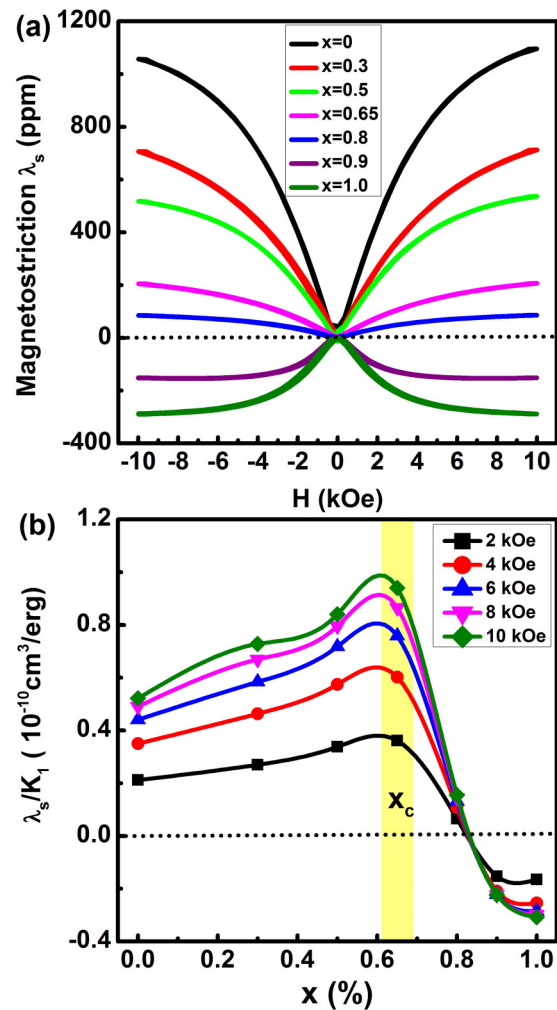

FIG. 6. Magnetostrictive measurements. (a) Magnetostriction (λ_S) for polycrystalline $Tb_{1-x}Nd_xCo_2$ alloys at 90 K under an applied magnetic field of 10 kOe. (b) Composition dependence of the ratio λ_S/K_1 for the $Tb_{1-x}Nd_xCo_2$ system.

upon magnetic ordering. Compared to a previously reported ferromagnetic $Tb_{1-x}Gd_xCo_2$ system involving MPB, lattice distortions of the two terminal compounds have the same level, resulting in a low net lattice distortion for the MPB composition of $Tb_{0.1}Gd_{0.9}Co_2$, and $TbCo_2$ with EMD along the $\langle111\rangle$ axis has a lower magnetization (M_S) than $GdCo_2$ with EMD along the $\langle100\rangle$ axis [15]. Therefore, MPB composition $x = 0.9$ tends to transform into the T phase. In $Tb_{1-x}Nd_xCo_2$, the magnitudes of lattice distortion of the two terminal compounds are different from each other, thus resulting in a low net lattice distortion near the MPB composition. Furthermore, $TbCo_2$ with $\langle111\rangle$ symmetry has a larger magnetization (M_S) than $NdCo_2$ with $\langle100\rangle$ symmetry. Therefore, under a large applied field, the MPB composition $x_c = 0.65$ tends to transform into the R phase.

IV. CONCLUDING REMARKS

Substitution of Tb with Nd shows a strong effect on the structural, magnetic, and magnetoelastic properties of $Tb_{1-x}Nd_xCo_2$. The synchrotron XRD results show that at

90 K the EMD of $Tb_{1-x}Nd_xCo_2$ lies along the $\langle 111 \rangle$ axis for $x < 0.65$ and changes to the $\langle 100 \rangle$ axis for $x > 0.65$. The saturation magnetization of $Tb_{1-x}Nd_xCo_2$ decreases with the increase of Nd concentration, exhibiting a minimum value near MPB $x_c = 0.65$. This can be ascribed to the compensation of antiparallel moments between Tb and Nd. The occurrence of SR can be attributed to the temperature dependence of magnetization, as described by a two-sublattice model. A detailed spin configuration diagram is provided for the $Tb_{1-x}Nd_xCo_2$ Laves phase around the composition for the anisotropy compensation; this can guide the development of novel magnetostrictive materials. The analysis of the synchrotron XRD and SR confirmed that the anisotropy compensation could be reached at the MPB composition $Tb_{0.35}Nd_{0.65}Co_2$, indicating that the substitution of Tb with Nd changes the anisotropic compensation point to the Nd-rich side. The decrease in magnetostriction with increasing Nd substitution can be ascribed to the decrease in λ_{111}. In addition, a low coercive field (H_C) under a low magnetic field and the large ratio between magnetostriction and the absolute values of the first anisotropy constant (λ_S / K_1) appears at MPB, i.e., $x_c = 0.65$, indicating that $Tb_{0.35}Nd_{0.65}Co_2$ has good magnetostrictive properties. This paper indicates the existence of MPB in ferromagnetic materials and suggests the differences between different ferromagnetic MPB systems that are important for substantial improvement of magnetic and magnetostrictive properties. Based on the results of this paper, similar MPB effects might be achieved in other ferroic systems that can be used for technological applications.

[1] S. B. Roy and P. Chaddah, Curr. Sci. **88**, 71 (2005).

[2] Z. W. Ouyang, F. W. Wang, Q. Huang, W. F. Liu, Y. G. Xiao, J. W. Lynn, J. K. Liang, and G. H. Rao, Phys. Rev. B **71**, 064405 (2005).

[3] V. K. Pecharsky and K. Gschneidner, Adv. Mater. **13**, 683 (2001).

[4] E. Gratz and A. Markosyan, J. Phys.: Condens. Matter **13**, R385 (2001).

[5] N. Baranov, E. Gratz, H. Nowotny, and W. Steiner, J. Magn. Magn. Mater. **37**, 206 (1983).

[6] R. Z. Levitin and A. S. Markosyan, Usp. Fiz. Nauk. **155**, 623 (1988).

[7] R. Z. Levitin and A. S. Markosyan, Sov. Phys. Usp. **31**, 730 (1988).

[8] R. Z. Levitin and A. S. Markosyan, J. Magn. Magn. Mater. **84**, 247 (1990).

[9] H. Klimker, M. Dariel, and M. Rosen, J. Phys. Chem. Solids **41**, 215 (1980).

[10] N. H. Duc and P. E. Brommer, *Handbook on Magnetic Materials* (North-Holland, Amsterdam, 1999).

[11] B. Jaffe, W. Cook, and H. Jaffe, *Piezoelectric Ceramics* (Academic, New York, 1971).

[12] M. Ahart, M. Somayazulu, R. Cohen, P. Ganesh, P. Dera, H. K. Mao, R. J. Hemley, Y. Ren, P. Liermann, and Z. Wu, Nature (London) **451**, 545 (2008).

[13] C. Zhou, W. Liu, D. Xue, X. Ren, H. Bao, J. Gao, and L. Zhang, Appl. Phys. Lett. **100**, 222910 (2012).

[14] S. Yang, H. Bao, C. Zhou, Y. Wang, X. Ren, Y. Matsushita, Y. Katsuya, M. Tanaka, K. Kobayashi, X. Song, and J. Gao, Phys. Rev. Lett. **104**, 197201 (2010).

[15] C. Zhou, S. Ren, H. Bao, S. Yang, Y. Yao, Y. Ji, X. Ren, Y. Matsushita, Y. Katsuya, M. Tanaka, and K. Kobayashi, Phys. Rev. B **89**, 100101 (2014).

[16] Z. W. Ouyang, F. W. Wang, Q. Hang, W. F. Liu, G. Y. Liu, J. W. Lynn, J. K. Liang, and G. H. Rao, J. Alloys Compd. **372**, 76 (2004).

[17] Y. Xiao, Q. Huang, Z. Ouyang, J. Lynn, J. Liang, and G. Rao, J. Alloys Compd. **420**, 29 (2006).

[18] Z. W. Ouyang, G. H. Rao, H. F. Yang, W. F. Liu, and J. K. Liang, Appl. Phys. Lett. **81**, 97 (2002).

[19] E. A. Sherstobitova, K. A. Kozlov, A. E. Teplykh, Yu. A. Dorofeev, Yu. N. Skryabin, and A. N. Pirogov, Crystallogr. Rep. **52**, 424 (2007).

[20] J. R. Cullen and A. E. Clark, Phys. Rev. B **15**, 4510 (1977).

[21] E. Gratz, A. Lindbaum, A. S. Markosyan, H. Mueller, and A. Y. Sokolov, J. Phys.: Condens. Matter **6**, 6699 (1994).

[22] N. Heiman, K. Lee, and R. I. Potter, in *Magnetism and Magnetic Materials*, edited by J. J. Becker, G. H. Lander, and J. J. Rhyne, AIP Conf. Proc. No. 29 (AIP, New York, 1994), p. 130.

[23] V. M. Goldberg, U. Atzmony, and M. P. Dariel, J. Mater. Sci. **15**, 127 (1980).

[24] A. Murtaza, S. Yang, C. Zhou, M. T. Khan, A. Ghani, F. Tian, J. Wang, X. Song, M. Suchomel, and Y. Ren, J. Alloys Compd. **680**, 177 (2016).

[25] Z.W.Ouyang, G. H. Rao, H. F. Yang, W. F. Liu, G. Y. Liu, X.M. Feng, and J. K. Liang, J. Phys.: Condens. Matter **15**, 2213 (2003).

[26] A. E. Clark, *Ferromagnetic Materials* (North-Holland, Amsterdam, 1980).

[27] J. A. Mydosh, *Spin Glasses: An Experimental Introduction* (Taylor & Francis, London, 1993).

[28] J. P. Liu, F. R. De. Boer, P. F. De. Chatel, R. Coehoorn, and K. H. J. Buschow, J. Magn. Magn. Mater. **132**, 159 (1994).

[29] Z. Z. dong, Z. Tong, P. F. De. Chatel, and F. R. De. Boer, J. Magn. Magn. Mater. **147**, 74 (1995).

[30] E. Y. Tsymbal and I. Zutic, *Handbook of Spin Transport and Magnetism* (Taylor & Francis, London, 2011).

[31] J. Rodríguez-Carvajal, Phys B.: Condens. Matter **192**, 55 (1993).

[32] R. Bergstrom, Jr., M. Wuttig, J. Cullen, P. Zavalij, R. Briber, C. Dennis, V. O. Garlea, and M. Laver, Phys. Rev. Lett. **111**, 017203 (2013).

[33] A. Murtaza, S. Yang, M. Mi, C. Zhou, J. Wang, R. Zhang, X. Liao, Y. Wang, X. Ren, X. Song, and Y. Ren, Appl. Phys. Lett. **106**, 132403 (2015).

[34] B. D. Cullity and C. D. Graham, *Introduction to Magnetic Materials* (Wiley, New York, 2011).

[35] Z. W. Ouyang, G. H. Rao, H. F. Yang, W. F. Liu, G. Y. Liu, M. H. Feng, and J. K. Liang, J. Alloys Compd. **390**, 21 (2005).

[36] Y. G. Shi, S. L. Tang, L. Y. Lv, and J. Y. Fan, J. Alloy Compd. **506**, 533 (2010).

[37] Y. G. Shi, X. G. Zhou, C. C. Hu, D. N. Shi, L. Y. Lv, and S. L. Tang, J. Alloys Compd. **581**, 753 (2013).